Influence of ethanol and temperature on adsorption of flavor-active esters on hydrophobic resins

Saffarionpour, Shima; Tam, Suk Ying S.; Van der Wielen, Luuk A.M.; Brouwer, Eric; Ottens, Marcel

DOI
10.1016/j.seppur.2018.05.026

Publication date
2019

Document Version
Final published version

Published in
Separation and Purification Technology

Separation and Purification Technology 210 (2019) 219–230

Contents lists available at ScienceDirect

Separation and Purification Technology

journal homepage: www.elsevier.com/locate/seppur

Influence of ethanol and temperature on adsorption of flavor-active esters on hydrophobic resins

Shima Saffarionpour[a], Suk-Ying S. Tam[a], Luuk A.M. Van der Wielen[a,1], Eric Brouwer[b], Marcel Ottens[a,*]

[a] Delft University of Technology, Department of Biotechnology, Van der Maasweg 9, 2629 HZ Delft, The Netherlands
[b] Heineken Supply Chain, Burgemeester Smeetsweg 1, 2382 PH Zoeterwoude, The Netherlands

ARTICLE INFO

Keywords:
Flavor-active esters
Adsorption
Ethanol
Temperature
Isosteric enthalpy

ABSTRACT

Flavor-active esters, produced during fermentation, are vital components and important contributors to the aroma of beer. In order to separate trace amounts of esters, their adsorption behavior in the presence of high concentrations of ethanol and their thermodynamic behavior under the influence of temperature needs to be understood. This study reports the influence of temperature on single component adsorption isotherms of four esters (i.e. ethyl acetate, isopentyl acetate, ethyl 4-methylpentanoate, and ethyl hexanoate) on two hydrophobic resins (i.e. Amberlite XAD16N, and Sepabeads SP20SS) and the estimation of heat, entropy, and Gibbs energy of adsorption. Higher heat and entropy of adsorption are obtained for ethyl hexanoate and ethyl 4-methylpentanoate in comparison, due to their higher hydrophobicity, stronger binding, and the exothermic nature of their adsorption. A higher concentration of ethanol (tested from 1 to 30% (v/v)), lowers the activity coefficient of esters in the aqueous phase, and subsequently lowers adsorption and Langmuir affinity parameters. Increase of temperature from 284.15 to 325.15 K shows a reverse influence on maximum adsorption capacity and Langmuir affinity parameters. Langmuir affinity parameters are obtained at various ethanol concentrations and temperatures. The reported parameters and thermodynamic properties in this paper, are essential for designing an industrial scale adsorption step for separation of flavor-active esters under non-isothermal conditions.

1. Introduction

Esters are volatile trace compounds which are present in fermented beverages like beer and are extremely important for the flavor profile of the final product [1–4]. Although esters are produced in trace amounts in comparison to other yeast metabolites, like higher alcohols, they are important aroma elements due to their low odour threshold in beverages [5–7]. They are responsible for the sweet and fruity flavors of beer [8,9] and if they are overproduced, they will negatively affect the final beer. Therefore, it is of importance to maintain optimum conditions to obtain a balanced ester profile in the final beer product [5,10]. These compounds are primarily formed during fermentation by enzymatic chemical condensation of organic acids and alcohols and are divided into two major groups of acetate esters and medium chain fatty acid ethyl esters [5,9–11]. While several esters are present in beer, the major ester components are considered to be ethyl acetate (solvent-aroma) [5,9,10], isopentyl acetate (banana aroma) [9,10,12], isobutyl acetate (fruity aroma) [5], phenyl ethyl acetate (rose and honey aroma) [9,10,13], ethyl hexanoate (sweet apple aroma) [9], ethyl 4-methylpentanoate (apple or pear aroma), and ethyl octanoate (sour apple aroma) [9]. During processing, however the level of esters and their relative concentrations might alter due to chemical and physical changes. In order to prevent the unwanted changes, esters can be selectively recovered and fractionated by means of adsorption and by tuning the level of esters present in different process streams various beer products with fruity flavors can be produced. Fractionation of esters in beer beverages can be challenging since they are present in the matrix at trace levels in comparison to ethanol, which is present at significant concentration. In order to design the adsorption process for selective recovery of esters, several process parameters, like the effect of ethanol on adsorption of esters and heat of adsorption for each specific compound in the mixture need to be understood. Therefore, this work aims to provide knowledge on the adsorption mechanism of flavor-active esters under the influence of temperature and various ethanol concentrations. Four major esters which contribute to beer flavor, i.e. ethyl acetate, isopentyl acetate, ethyl hexanoate and ethyl 4-

* Corresponding author.
E-mail address: m.ottens@tudelft.nl (M. Ottens).
[1] Bernal Institute, University of Limerick, Limerick, Ireland.

https://doi.org/10.1016/j.seppur.2018.05.026
Received 26 January 2018; Received in revised form 7 May 2018; Accepted 13 May 2018
Available online 18 May 2018

Nomenclature

C	equilibrium concentration (mmol/L)
ΔH_s	isosteric heat of adsorption (kJ/mol)
T	temperature (K)
R	gas constant (J/(mol K))
q	adsorption capacity (mmol/L)
q_{max}	maximum load (mmol/L)
$k_{ads,L}$	Langmuir parameter (L/mmol)
$k_{ads,s}$	sips parameter $(mmol/L)^{(-1/n)}$
K	Langmuir equilibrium constant (–)
k_∞	Langmuir temperature independent factor (L/mmol)
ΔH^0	heat of adsorption (kJ/mol)
n	sips parameter (–)
k_0	adsorption affinity at reference temperature (L/mmol)
n_0	sips parameter at reference temperature (–)
T_0	reference temperature (K)
$q_{max,0}$	saturation capacity at reference temperature (mmol/L)
Q	isosteric heat at $\theta = 1/2$ (kJ/mol)
ΔG^0	Gibbs energy of adsorption (kJ/mol)
ΔS^0	entropy of adsorption (kJ/mol)
M_{init}	moles of analyte in initial sample (mmol)
C_0	initial molar concentration (mmol/L)
V_0	initial volume of analyte (L)
M_{bulk}	moles of analyte in bulk solution (mmol)
C_{blank}	concentration blank (mmol/L)
V_{blank}	volume blank (L)
m_{resin}	mass of wet resin (g)
$K_{affinity}$	Langmuir affinity parameter (L/g)

Greek symbols

θ	fractional coverage (–)
α	sips constant parameter (–)
χ	constant parameter for temperature dependent q_{max} (–)

methylpentanoate are selected and the adsorption of aforementioned esters is investigated on the synthetic hydrophobic resins, Sepabeads SP20SS and Amberlite XAD16N, which showed high affinity towards esters according to our previous investigations, both for single and multi-compound mixtures [14]. The uptake on each resin is examined at different concentrations of ethanol and the influence of temperature on adsorption of single and multi-component mixture of esters is explored. Based on the acquired results, the thermodynamic properties such as the heat, entropy, and Gibbs energy of adsorption for each specific ester present in the mixture are calculated and affinity of each resin towards the tested esters at various ethanol concentrations and temperatures is obtained. The estimated thermodynamic properties and the obtained affinity parameters have application in designing the adsorption column for selective recovery of flavor-active esters.

2. Materials

2.1. Chemicals

Ethyl acetate (purity ≥ 99.5%), isopentyl acetate (98%), ethyl hexanoate, and ethyl 4-methylpentanoate are purchased from Sigma-Aldrich, The Netherlands. MilliQ water is used for dilutions and ethanol 96%, is purchased from Merck.

2.2. Adsorbents

Food grade resin XAD16N from Amberlite resin series and the aromatic type Sepabeads SP20SS from HP resin series are purchased from Sigma-Aldrich, The Netherlands and used for adsorption tests. Detailed specifications and physical properties of the tested resins are reported in our previous work [14].

3. Methods

3.1. Gas chromatographic analysis

The esters of interest were analyzed by Static-Headspace-Gas-Chromatography (HS-GC) method using the GC (Trace 1300, Thermofischer Scientific, Switzerland) coupled with Triplus RSH Autosampler (Thermofischer Scientific, Switzerland) and FID in a RESTEK Rxi 624Sil MS column (20 mm × 0.18 mm *ID* × 1 µm *df*), (Restek Co., US) Helium was used as the carrier gas in the system. The incubation temperature of the GC agitator was set to 40 °C and samples were measured with incubation time of 20 min. Syringe temperature was set to 60 °C and detector temperature to 250 °C. Instead of direct injection of the vapor to the GC column, injection is performed through a GC splitting inlet, which aids obtaining sharper peaks and reduces the amount of sample reaching the GC column. Split ratio of 30 was used for the measurements. Ramped oven temperature was considered for the GC settings, 60 °C with holding time of 1 min, increase to 75 °C with the increasing rate of 10 °C/min, and the second increase to 175 °C with the speed of 30 °C/min with the holding time of 1 min. The retention time of tested components is measured during 7 min analysis time. The chromatograms obtained from the measurements show the retention time (minutes) of 1.5, 2.4, 4.9, 5.5, and 5.7 for ethanol, ethyl acetate, isopentyl acetate, ethyl 4-methylpentanoate, and ethyl hexanoate respectively.

3.2. Thermodynamic analysis

3.2.1. Selection of isotherm models

An extensive isotherm study was performed in our previous work in order to express the adsorption behavior of components, which belong to the group of esters, higher alcohols, and diketones [14]. Among the availabale and proposed models reported in the literature, Langmuir, Freundlich, and Sips (Langmuir-Freundlich) models were selected as the most appropriate models for expression of the equilibrium data.

Results of the tests revealed high accuracy in prediction with Langmuir and Sips models, therefore the previously tested models are selected to explain the adsorption behavior of flavor-active esters for this study and Langmuir and Sips models, which were able to predict the experimental adsorption equilibrium data with higher accuracy are further investigated for determination of isosteric enthalpy of adsorption in the next step.

3.2.1.1. Langmuir isotherm. The simplest model, which describes the monolayer adsorption, is the Langmuir model. This model works under the assumption that the resin surface consists of several different regions and each region follows the Langmuir assumption that one molecule is adsorbed to one site, homogeneous surface and a localized adsorption [15,16]. This model can be explained as is shown in Eq. (1).

$$\theta = \frac{q}{q_{max}} = \frac{k_{ads,L}C}{1 + k_{ads,L}C} \tag{1}$$

where θ is the fractional coverage (–), q and q_{max} are the adsorption capacity, and maximum load respectively (mmol/L), $k_{ads,L}$ is the Langmuir constant (L/mmol), and C is the equilibrium concentration of the analyte (mmol/L).

3.2.1.2. Freundlich isotherm. This empirical isotherm model describes the adsorption capacity as a function of adsorbate concentration with a

logarithmic scale as is described in Eq. (2).

$$q = K_f C^{1/n} \tag{2}$$

where K_f is the maximum capacity $(\text{mmol/L})^{(-1/n)}$ and 1/n is the adsorption intensity.

3.2.1.3. Sips isotherm. The Sips model is the combined form of Langmuir and Freundlich model. It circumvents the limitation of increase in adsorbate concentration (with power 1/n), which is associated with the Freundlich model and makes it possible to achieve an improved fit at high concentrations [14,17,18]. This isotherm model can be written in the generalized form, shown in Eq. (3).

$$\theta = \frac{q}{q_{max}} = \frac{(k_{ads,s}C)^{1/n}}{1 + (k_{ads,s}C)^{1/n}} \tag{3}$$

where $k_{ads,S}$ is the Sips constant $(\text{mmol/L})^{(-1/n)}$.

3.2.2. Determination of adsorption isosteric enthalpy

Isosteric enthalpy, which is the basic quantity in adsorption study, is explained as the ratio of the infinitesimal change in the adsorbate enthalpy to the infinitesimal change in the amount adsorbed. When heat is released due to adsorption, part of the released energy is adsorbed by the solid adsorbent and it is partly dissipated into the surrounding. The heat adsorbed by the solid particle increases the particle temperature, therefore it is of importance to understand and quantify the amount of the isosteric enthalpy for further studies. The amount of this heat can be calculated based on Van't Hoff relation, as explained in Eq. (4) [19–25].

$$-\left(\frac{\partial \ln C}{\partial T}\right)_q = \frac{\Delta H_s}{RT^2} \tag{4}$$

where ΔH_s is the isosteric enthalpy of adsorption, kJ/mol, R is the gas constant (8.314 J/mol K), T is the temperature in K, and C is the equilibrium concentration (mmol/L) [15,16,26].

3.2.2.1. Langmuir approach. The Langmuir expression explained in Section 3.2.1.1, Eq. (1), shows monolayer adsorption since

$$(C \to \infty), (q \to q_{max}), \theta \to 1,$$

while at low concentrations of the analyte, Henry's approach will follow, which can be explained as Eq. (5) [16,27]

$$\lim_{C \to 0}\left(\frac{q}{C}\right) = k_{ads,L} q_{max} = K \tag{5}$$

q_{max} represents a fixed number of surface sites and is independent of temperature. However, the Langmuir constant is dependent on temperature as is explained by Arrhenius equation, presented in Eq. (6) [28,29].

$$k_{ads,L} = k_\infty \exp\left(-\frac{\Delta H_s}{RT}\right) \tag{6}$$

k_∞ is the temperature-independent factor (L/mmol), ΔH_s is the isosteric enthalpy of adsorption (kJ/mol) which in this case is assumed to be equal to heat of adsorption [15], R is the gas constant (J/mol K) and T is the temperature (K). The magnitude of the heat of adsorption indicates the dominant type of adsorption (physical or chemical). The heat of adsorption for physisorption process is between 5 and 40 kJ/mol while higher heat of adsorption can be achieved in chemisorption (40–800 kJ/mol) [29,30]. If the adsorption process is exothermic and q_{max} decreases with temperature, the heat of adsorption will increase with the loading and if the isosteric enthalpy has a finite value at high coverage, the saturation capacity is independent of temperature and heat of adsorption will be constant [15]. Then Eq. (4) can be rewritten as explained in Eq. (7) [16].

$$-\left(\frac{\partial \ln C}{\partial T}\right)_q = \frac{\Delta H_s}{RT^2} = \frac{d \ln K}{RT^2} = \frac{\Delta H^0}{RT^2} \tag{7}$$

where ΔH^0 is the heat of adsorption (kJ/mol).

3.2.2.2. Sips approach. For the sips mode, explained in Section 3.2.1.3, the constant $k_{ads,s}$ and the exponent n, temperature dependency can be considered in the next equations,

$$k_{ads,s} = k_\infty \exp\left(\frac{-\Delta H_s}{RT}\right) = k_0 \exp\left[\frac{-\Delta H_s}{RT_0}\left(\frac{T_0}{T} - 1\right)\right] \tag{8}$$

$$\frac{1}{n} = \frac{1}{n_0} + \alpha\left(1 - \frac{T_0}{T}\right) \tag{9}$$

where k_∞ is the adsorption affinity constant, k_0 is that at reference temperature T_0, n_0 is the same parameter n at the same reference temperature and α is a constant parameter. Unlike ΔH_sin the Langmuir equation, where it is equal to the isosteric enthalpy, this parameter can only express the heat of adsorption in the Sips equation and the temperature dependency of exponent n needs to be considered. The maximum saturation capacity can be considered as constant or it can be expressed as is shown in Eq. (10), the choice of this temperature dependency is arbitrary [15].

$$q_{max} = q_{max,0} \exp\left[\chi\left(1 - \frac{T}{T_0}\right)\right] \tag{10}$$

$q_{max,\,o}$ is the saturation capacity at the reference temperature T_O and χ is a constant parameter. q_{max} can be considered as temperature dependent, or the term χ can be set to zero [15]. In order to obtain the isosteric enthalpy for the temperature dependence form of the Sips equation from the Van't Hoff relation, and considering temperature dependence of $k_{ads,s}$, and $1/n$, the isosteric enthalpy can be written as explained in Eq. (11) [15].

$$-\Delta H_s = Q - (\alpha R T_0) n^2 \ln\left(\frac{\theta}{1-\theta}\right) \tag{11}$$

With the assumption that temperature variation of q_{max} is negligible. It can be observed from Eq. (11) that the isosteric enthalpy decreases with loading. When the loading is equal to zero, it goes to infinity and when it reaches the saturation point, it approaches minus infinity.

Although this model is capable to predict the final maximum capacity with accuracy at high concentrations, for accurate estimation of heat of adsorption, it is only applicable for intermediate range of concentrations [15].

The physical meaning of parameter Q is explained in Eq. (12). At fractional coverage equal to one half, the isosteric enthalpy is equal to the value of Q (kJ/mol) [15].

$$Q = (-\Delta H_s)|_{\theta = 1/2} \tag{12}$$

3.2.3. Determination of Gibbs energy (ΔG^0) from Langmuir constant

The Gibbs energy change indicates the degree of spontaneity of the adsorption process. The higher negative value indicates a more favorable adsorption. The amount of change in Gibbs energy can be calculated according to Eq. (13), from Langmuir constant K [23,27,31].

$$\Delta G^0 = -RT \ln K \tag{13}$$

where K is the Langmuir equilibrium constant (q/C) and is dimensionless, T is the absolute temperature (K) and R is the gas constant (8.314 J/mol K).

3.2.4. Determination of heat (ΔH^0) and entropy (ΔS^0) of adsorption

The Gibbs free energy change is related to the heat (ΔH^0) and entropy change (ΔS^0) of adsorption which the relation can be expressed as Eq. (14) [16,23,32,33].

$$\ln K = \frac{\Delta S^0}{R} - \frac{\Delta H^0}{RT} \quad (14)$$

where K is the dimensionless equilibrium constant (–). The values of heat of adsorption (ΔH^0) and entropy change of adsorption (ΔS^0) can be calculated from the slope and intercept of the Van't Hoff plot, ln K versus the $(1/T)$ [33–35].

3.2.5. Determination of competitive adsorption parameters

3.2.5.1. Multicomponent Langmuir approach. For designing an adsorption column at an industrial scale for separation and fractionation of flavor-active esters which are present in different process streams with large amounts of ethanol, the competitive adsorption behavior of these compounds present with various concentrations of ethanol and at different temperatures needs to be investigated. In order to study the adsorption behavior and obtain the required parameters for the design stage, a multi-component Langmuir model is used to express the experimental data collected from adsorption tests performed through batch uptake experimentation at different concentrations of ethanol and at various temperatures. The extension of the Langmuir model, which describes the competition of component i with nc components in the mixture, is used to express the experimental data (see Eq. (15)) [14,36–39].

$$q_i = \frac{q_{max} k_{ads,i} C_i}{1 + \sum_{j=1}^{nc} k_{ads,j} C_j} \quad (15)$$

where C_i represents the concentration in the bulk liquid of species i at equilibrium condition (mg/L), q_i is the load of species i (concentration of adsorbate on solid) (mg/g_{resin}), q_{max} represents the maximum load (mg/g_{esin}), and $k_{ads,i}$ is the Langmuir constant (L/mg). $K_{affinity}$ (L/g_{resin}) can be obtained through multiplication of $k_{ads,i}$ by q_{max}.

3.3. Batch uptake method

Batch uptake experimentation is used for testing the adsorption behavior of selected esters on the two synthetic hydrophobic resins. Experiments are performed in 10 ml clear crimp top headspace vials (Thermofischer Scientific, Switzerland), which were filled with the selected resins after the resin preparation step. Since resins are rather hydrophobic, they are prepared through washing steps with methanol, followed by an equilibration step with water and addition of the resins to each vial. Afterwards, different concentrations of the solution are added to the vials and closed with Crimpcap Bi-metal septum 20 mm (Thermofischer Scientific, Switzerland) to prevent evaporation. Vials are stirred at 500 rpm for one hour equilibration time on a thermo-mixer (comfort Eppendorf, Hamburg, Germany) at different temperatures tested for the experiments. After equilibration, bulk liquid is filtered using the Millex-HV low binding syringe filter unit, 0.45 µm, PVDF, 33 mm (Merck Millipore, The Netherlands) through 5 ml syringe in the 10 ml headspace vial and closed with metal caps, prepared for the analysis.

The amount of solute i adsorbed per unit mass on adsorbate (q_i) is calculated using the mass balance (Eq. (16)) [40].

$$q_i = \frac{M_{init} - M_{bulk} - M_{lost,evap}}{m_{resin}} \quad (16)$$

where M_{init} is the initial number of moles of the analyte in the solution (mmol), calculated from the initial molar concentration and initial sample volume $C_0 V_0$ where C_0 is the initial molar concentration (mmol/L), and V_0 is the initial volume of the analyte (L). M_{bulk} is the number of moles of the bulk liquid remained after adsorption (mmol). In order to take into account the effect of evaporation, the amount of moles of the analyte which are lost due to evaporation are considered in the estimation of the equilibrium capacity which can be estimated from $(C_0 V_0 - C_{blank} V_{blank})$, where V_{blank} is the volume of the blank samples after the equilibration time. The value of m_{resin} is the gram of the wet resin.

3.4. Experimental procedure

3.4.1. Single-component adsorption test

Batch uptake experiments are performed to investigate the adsorption of the flavor-active esters on two hydrophobic resins Sepabeads SP20SS and Amberlite XAD16N. Approximately 0.4 g/L of the flavor-active esters, i.e. ethyl acetate, isopentyl acetate, ethyl hexanoate, and ethyl 4-methylpentanoate are prepared in 1% (v/v) co-solvent mixture of ethanol/water. Batch uptake experimentation, is applied as explained in Section 3.3 to investigate the single-component adsorption of the aforementioned components. The adsorption experiments are performed at four different tested temperatures (i.e. 284.15, 297.15, 309.15, and 333.15 K).

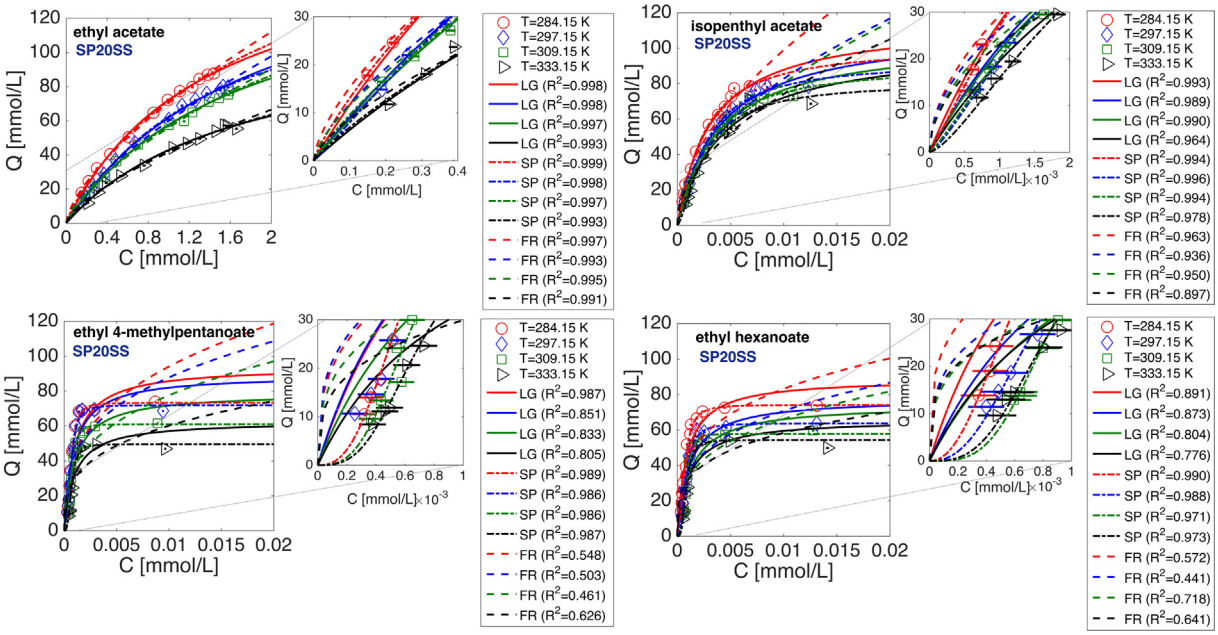

Fig. 1. Adsorption isotherms for tested esters at four temperatures, prediction based on Langmuir (LG), Freundlich (FR), and Sips (SP) models; Adsorption on Sepabeads SP20SS.

3.4.2. Multi-component adsorption tests

Ester components are present in trace amounts in comparison to ethanol, which is present at higher concentration range. In order to investigate the competitive adsorption of esters, studying the influence of temperature and ethanol concentration on their binding capacity is required; therefore, the competitive adsorption of flavor-active esters is investigated through batch uptake experimentation according to the procedure explained in Section 3.3. Approximately 0.4 g/L of each flavor-active ester is prepared in co-solvent mixture of ethanol/water. Experiments are performed over wide range of ethanol concentration (i.e. 1, 7.5, 15, 22.5, and 30% (v/v)) and at three different temperatures (i.e. 284.15, 297.15, and 325.15 K).

4. Results and discussions

4.1. Influence of temperature on single-component adsorption

4.1.1. Single-component adsorption isotherms

The results of the adsorption isotherms at four different tested temperatures, are illustrated in Fig. 1 for adsorption of the flavor-active esters on Sepabeads SP20SS resin and for the four tested esters. The adsorption equilibrium data are explained with single-component Langmuir, Freundlich, and Sips models. As can be observed from Fig. 1, the increase of temperature is not favorable for adsorption, due to exothermic nature of adsorption, and a decrease in the amount of maximum capacity at saturation point is observed. Comparing the results obtained for four tested esters, i.e. ethyl acetate, isopentyl acetate, ethyl 4-methylpentanoate, and ethyl hexanoate, it can be concluded that the resin SP20SS, has higher affinity towards the tested components in the order of their hydrophobicity, ethyl hexanoate as the most hydrophobic compound, followed by ethyl 4-methylpentanoate, isopentyl acetate, and ethyl acetate. The degree of hydrophobicity can be explained by the value of log P (Partition coefficient in octanol/water solution), which has the value of 2.31, 2.16, 1.53, and 0.28 for ethyl hexanoate, ethyl 4-methylpentanoate, isopentyl acetate, and ethyl acetate respectively [41]. By comparing the four figures for the tested esters, it can be clearly observed that ethyl hexanoate has more tendency to bind to the resin material, and the least bulk concentration remained after adsorption is obtained for this component. The value of equilibrium bulk concentration increases as the hydrophobicity of the molecule decreases and less analyte is adsorbed on the resin material.

Comparison of the Langmuir, Freundlich, and Sips fit for the four tested esters presented in Fig. 1, neatly demonstrate that high accuracy in prediction can be obtained for ethyl acetate by Langmuir, and Sips models (values of R^2 higher than 0.993). Prediction for adsorption behavior of isopentyl acetate, ethyl 4-methylpentanoate, and ethyl hexanoate obtained based on Langmuir model, is improved, specifically at the saturation point and lower concentration region through Sips model, as the higher values of R^2 demonstrate. This model combines the behavior of Freundlich and Langmuir model and circumvents the limitation of rising adsorbate concentration associated with the Langmuir model which is observed here [14,42]. Freundlich model was not able to predict the adsorption behavior with high accuracy; lower values of R^2 obtained specially for ethyl 4-methylpentanoate and ethyl hexanoate. This model has the drawback that it cannot be applied with high accuracy for prediction of maximum saturation point due to increase in concentration with power 1/n.

The results of single-component adsorption tests obtained in the similar condition for the four tested esters and on Amberlite XAD16N resin are presented in Fig. 2. More accurate prediction based on Langmuir model is obtained for the two components with the highest hydrophobicity (i.e. ethyl 4-methylpentanoate and ethyl hexanoate) in comparison to the predictions obtained for adsorption on SP20SS (higher values of R^2). The pore volume of XAD16N resin is smaller than SP20SS (0.55 in comparison to 1.01 ml/g) [43,44] and the adsorption phenomena is less dominated by pore diffusion on this resin, therefore components with higher hydrophobicity, have less tendency to bind strongly to the resin in comparison to SP20SS and adsorption isotherms can be described more accurately by Langmuir model and monolayer adsorption. From the obtained results and isotherms, it can be concluded that Langmuir model is able to predict the adsorption behavior of flavor-active esters with accuracy. This prediction can be improved through Sips model, specifically for the components with high hydrophobicity, therefore these two models are selected to be studied for determination of heat of adsorption. Due to low accuracy in prediction with the Freundlich model, this model is not selected for further study.

4.1.2. Heat of adsorption (ΔH^0)

4.1.2.1. Determination based on Langmuir model. Based on the obtained isotherms at four different temperatures, the values of maximum

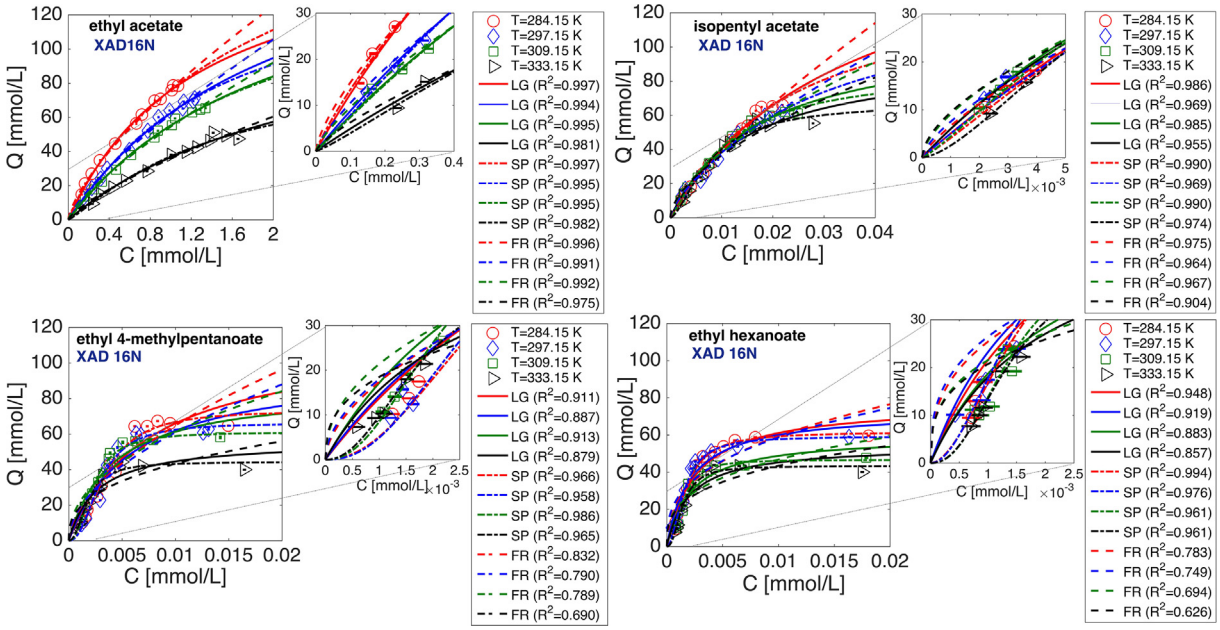

Fig. 2. Adsorption isotherms for tested esters at four temperatures, prediction based on Langmuir (LG), Freundlich (FR), and Sips (SP) models; Adsorption on Amberlite XAD16N.

Table 1
Regressed parameters for adsorption on Sepabeads SP20SS, based on temperature dependent Langmuir model. All parameters are given with their 95% confidence bounds.

	Temperature (K)			
	284.15 K	297.15 K	309.15 K	333.15 K
Ethyl acetate				
q_{max} (mmol L^{-1})	172.5 (157.6, 187.4)	176.6 (159.7, 193.4)	161.1 (141.9, 180.3)	117.8 (99.1, 136.5)
k_∞ (L $mmol^{-1}$)	0.0023 (0.0019, 0.0026)	0.0021 (0.0018, 0.0025)	0.0025 (0.0020, 0.0030)	0.0045 (0.0032, 0.0057)
$(-\Delta H^0)$ (kJ/mol)	−13.614 (−13.612, −13.615)	−13.657 (−13.655, −13.658)	−13.851 (−13.850, −13.852)	−13.441 (−13.440, −13.442)
Isopentyl acetate				
q_{max} (mmol L^{-1})	115.6 (105.5, 125.8)	112.0 (100.7, 123.3)	105.9 (95.5, 116.4)	102.8 (82.5, 123.1)
k_∞ (L $mmol^{-1}$)	0.0104 (0.0082, 0.0125)	0.0110 (0.0084, 0.0137)	0.0158 (0.0122, 0.0195)	0.0188 (0.0104, 0.0272)
$(-\Delta H^0)$ (kJ/mol)	−24.375 (−24.373, −24.375)	−24.794 (−24.793, −24.795)	−24.925 (−24.924, −24.925)	−26.104 (−26.103, −26.104)
Ethyl 4-methylpentanoate				
Q_{max} (mmol L^{-1})	94.1 (68.0, 120.2)	89.3 (64.8, 113.7)	78.9 (56.3, 101.6)	62.7 (43.2, 82.1)
k_∞ (L $mmol^{-1}$)	0.0099 (0.0034, 0.0164)	0.0080 (0.0026, 0.0135)	0.0239 (0.0075, 0.0402)	0.0325 (0.0077, 0.0573)
$(-\Delta H^0)$ (kJ/mol)	−27.253 (−27.253, −27.253)	−29.266 (−29.265, −29.266)	−27.315 (−27.314, −27.315)	−28.661 (−28.660, −28, 661)
Ethyl hexanoate				
Q_{max} (mmol L^{-1})	88.9 (71.8, 106.1)	77.8 (60.4, 95.2)	74.4 (52.9, 95.8)	65.8 (45.9, 85.7)
k_∞ (L $mmol^{-1}$)	0.0038 (0.0018.0.0058)	0.0045 (0.0019, 0.0071)	0.0053 (0.0016, 0.0090)	0.0084 (0.0017, 0.0150)
$(-\Delta H^0)$ (kJ/mol)	−29.719 (−29.719, −29.719)	−30.129 (−30.128, −30.129)	−30.607 (−30.606, −30.607)	−32.196 (−32.195, −32.196)

Table 2
Regressed parameters for adsorption on Amberlite XAD16N, based on temperature dependent Langmuir model. All parameters are given with their 95% confidence bounds.

	Temperature (K)			
	284.15 K	297.15 K	309.15 K	333.15 K
Ethyl acetate				
q_{max} (mmol L^{-1})	191.9 (130.4, 253.5)	199.9 (141.2, 258.5)	182.6 (142.7, 222.6)	131.9 (80.9, 182.9)
k_∞ (L $mmol^{-1}$)	0.0033 (0.0016, 0.0049)	0.0030 (0.0017, 0.0043)	0.0033 (0.0023, 0.0043)	0.0037 (0.0016, 0.0059)
$(-\Delta H^0)$ (kJ/mol)	−12.567 (−12.566, −12.567)	−12.368 (−12.368, −12.368)	−12.508 (−12.507, −12.508)	−12.825 (−12.824, −12.825)
Isopentyl acetate				
q_{max} (mmol L^{-1})	183.2 (123.8, 242.6)	139.0 (101.5, 176.5)	119.2 (91.3, 147.2)	96.6 (68.3, 124.9)
k_∞ (L $mmol^{-1}$)	0.0053 (0.0028, 0.0078)	0.0084 (0.0047, 0.0120)	0.0180 (0.0106, 0.0254)	0.0456 (0.0198, 0.0715)
$(-\Delta H^0)$ (kJ/mol)	−20.238(−20.236, −20.238)	−20.761 (−20.760, −20.762)	−20.326 (−20.325, −20.327)	−20.134 (−20.133, −20.135)
Ethyl 4-methylpentanoate				
q_{max} (mmol L^{-1})	114.6 (69.0, 160.3)	98.2 (61.5, 134.8)	85.9 (62.2, 109.5)	56.3 (40.7, 71.8)
k_∞ (L $mmol^{-1}$)	0.0163 (0.0041, 0.0285)	0.0337 (0.0082, 0.0592)	0.0707 (0.0279, 0.1134)	0.1966 (0.0626, 0.3306)
$(-\Delta H^0)$ (kJ/mol)	−21.304 (−21.302, −21.305)	−21.058 (−21.057, −21.059)	−20.976 (−20.975, −20.976)	−20.955 (−20.953, −20.956)
Ethyl hexanoate				
q_{max} (mmol L^{-1})	76.7 (63.8, 89.6)	72.8 (58.4, 87.3)	59.4 (45.6, 73.2)	54.4 (39.81, 68.9)
k_∞ (L $mmol^{-1}$)	5.0788e−4 (2.8327e−4, 7.3250e−4)	0.0010 (5.1270e−4, 0.0015)	0.0041 (0.0017, 0.0064)	0.0086 (0.0026, 0.0145)
$(-\Delta H^0)$ (kJ/mol)	−32.001 (−32.000, −32.001)	−32.250 (−32.249, −32.250)	−29.899 (−20.898, −20.899)	−30.359 (−30.358, −30.359)

capacity (q_{max}), the temperature independent factor (k_∞), and heat of adsorption ΔH^0 are regressed using the *nlinfit* function in MATLAB, for the temperature dependent Langmuir model, explained in Section 3.2.1.1. The values of 95% confidence intervals for the nonlinear least squares parameter estimates, are estimated based on coefficient covariance matrix and the toolbox *nlparci* [45,46] in MATLAB. The calculated parameters, based on the temperature dependent Langmuir model, (substituting Eq. (6) in Eq. (1)), are assembled in Tables 1 and 2, for adsorption on Sepabeads SP20SS and Amberlite XAD16N respectively.

The estimated heats of adsorption, reveal that the adsorption is an exothermic phenomenon and the increase of temperature is not favorable for adsorption. The regressed values for maximum capacities, for four tested esters show that, increase of temperature has a reverse influence on the value of maximum capacity, as the value for q_{max} decreases with temperature increase. The higher value for heat of adsorption is expected for higher hydrophobic components, (i.e. ethyl hexanoate and ethyl 4-methylpentanoate) since they interact and compete more for binding to the resin material and there is a higher energy barrier that adsorbed molecules need to overcome to leave the adsorbed phase [15]. The estimated values for heat of adsorption, for ethyl acetate is below 20 kJ/mol and it indicates that the adsorption is mainly dominated by physisorption for this component, since the value of ΔH^0 for physical adsorption is the same order of magnitude as condensation (i.e. 2.1–20.9 kJ/mol) [47,48] as extensively reported in the literature. If the value for heat of adsorption lies between 80 and 200 kJ/mol, the adsorption phenomena is mainly dominated by chemisorption [47,48].

The calculated values for enthalpies of adsorption, for the other three hydrophobic components, are above 20 kJ/mol and below 80 kJ/mol, and they imply that simultaneous physical and chemical adsorption occur for esters with higher hydrophobicity as they bind stronger to the adsorbent.

Similar procedure is followed to obtain the parameters for adsorption on Amberlite XAD16N resin. The regressed values for this tested resin are reported in Table 2. Lower value for heat of adsorption, is obtained for adsorption of three hydrophobic esters, i.e. isopentyl acetate, ethyl 4-methylpentanoate and ethyl hexanoate, on this resin in comparison to Sepabeads SP20SS. The observed trend can be explained by the nature of the adsorbent materials, since Sepabeads SP20SS has

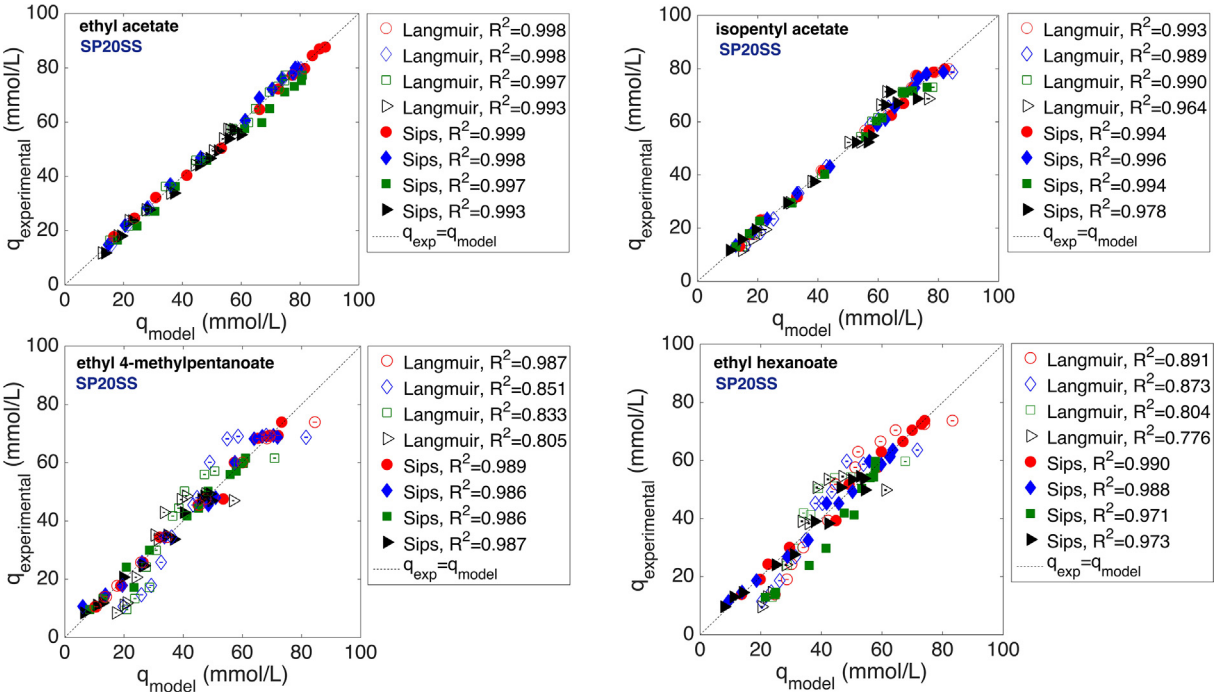

Fig. 3. Parity plot q_{model} (Predicted based on Langmuir and Sips models) vs. $q_{experimental}$; Adsorption on Sepabeads SP20SS (○● 284.15 K, ◇♦ 297.15 K, □■ 309.15 K, ▷▶ 333.15 K).

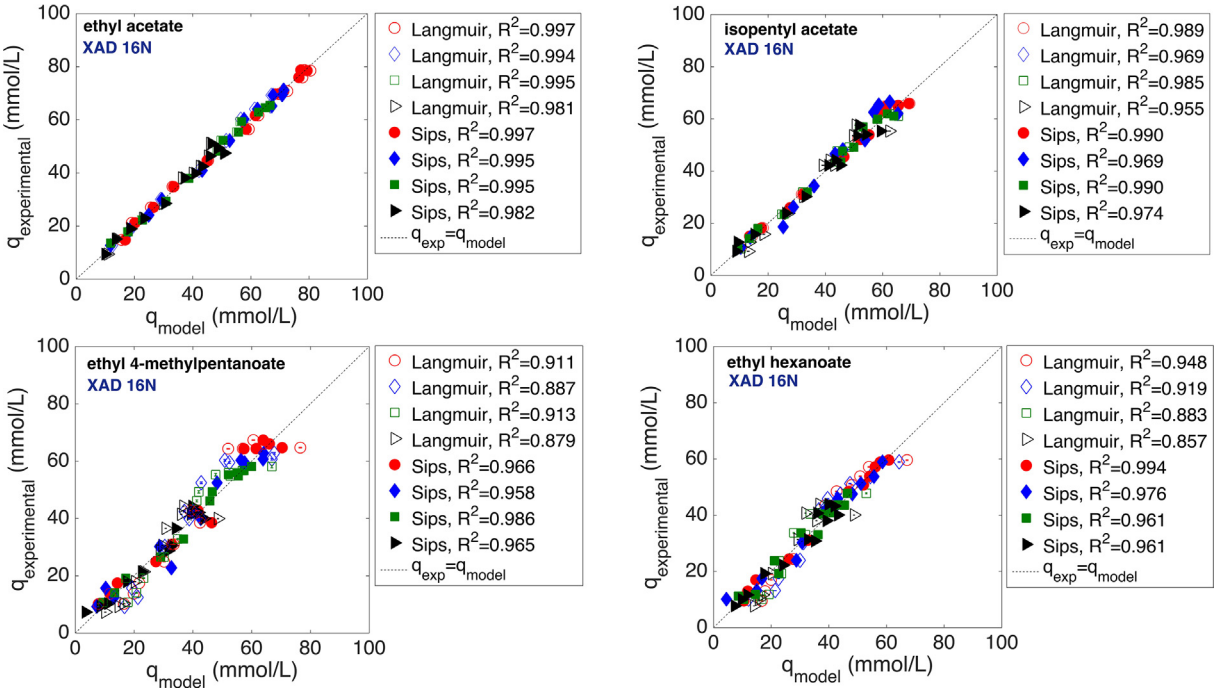

Fig. 4. Parity plot q_{model} (Predicted based on Langmuir and Sips models) vs. $q_{experimental}$; Adsorption on Amberlite XAD16N (○● 284.15 K, ◇♦ 297.15 K, □■ 309.15 K, ▷▶ 333.15 K).

smaller particle size and larger pore volume in comparison, it has higher affinity towards the high hydrophobic esters and more heat is released after their adsorption.

Based on the regressed parameters, the value for $k_{ads,L}$ is estimated from calculated heats of adsorption according to Eq. (6) and subsequently the equilibrium binding capacity is calculated from Eq. (1), knowing the maximum binding capacity for each tested ester. The values of equilibrium binding capacity, predicted by the temperature dependent Langmuir model and the values obtained from experiments are compared in a parity plot for each ester and for adsorption on two tested hydrophobic resins, i.e. SP20SS, and XAD16N, presented in Figs. 3 and 4.

The presented results in Figs. 3 and 4 confirm the behavior observed in Figs. 1 and 2 and reveal improvement in prediction through Sips model, specifically at low concentration region.

4.1.2.2. Determination based on Sips model. It is shown in Figs. 1–4 and explained in Section 4.1.1, that the Sips model has advantages in

Table 3
Regressed parameters for estimation of isosteric enthalpy of ethyl acetate based on Sips model.

	Temperature (K)			
	284.15 K	297.15 K	309.15 K	333.15 K
Sepabeads Sp20SS				
$q_{max,0}$ (mmol/L)	266.215 ± 0.004	146.756 ± 0.008	210.172 ± 0.007	140.39 ± 0.011
k_0 (mmol/L)$^{-1/n}$	0.461 ± 2.147	1.184 ± 1.112	0.739 ± 1.872	1.249 ± 1.285
Q (kJ/mol)	13.299 ± 0.074	13.278 ± 0.122	13.280 ± 0.1042	13.284 ± 0.121
n_0 (–)	1.231 ± 0.803	0.959 ± 1.188	1.271 ± 1.088	1.286 ± 1.248
α (–)	0.8209 ± 1.205	0.733 ± 1.419	0.986 ± 1.402	0.825 ± 1.946
$(-\Delta H_s\|_{\theta=1/2})$ (kJ/mol)	**13.3**			
Amberlite XAD16N				
$q_{max,0}$ (mmol/L)	240.454 ± 0.006	147.761 ± 0.012	157.248 ± 0.009	92.077 ± 0.0235
k_0 (mmol/L)$^{-1/n}$	0.578 ± 2.339	0.464 ± 3.699	0.278 ± 5.169	0.240 ± 9.008
Q (kJ/mol)	13.063 ± 0.103	13.063 ± 0.131	13.060 ± 0.110	13.067 ± 0.166
n_0 (–)	1.166 ± 1.159	0.953 ± 1.799	1.068 ± 1.344	0.964 ± 2.247
α (–)	0.946 ± 1.428	0.879 ± 1.949	0.915 ± 1.569	0.801 ± 2.702
$(-\Delta H_s\|_{\theta=1/2})$ (kJ/mol)	**13.1**			

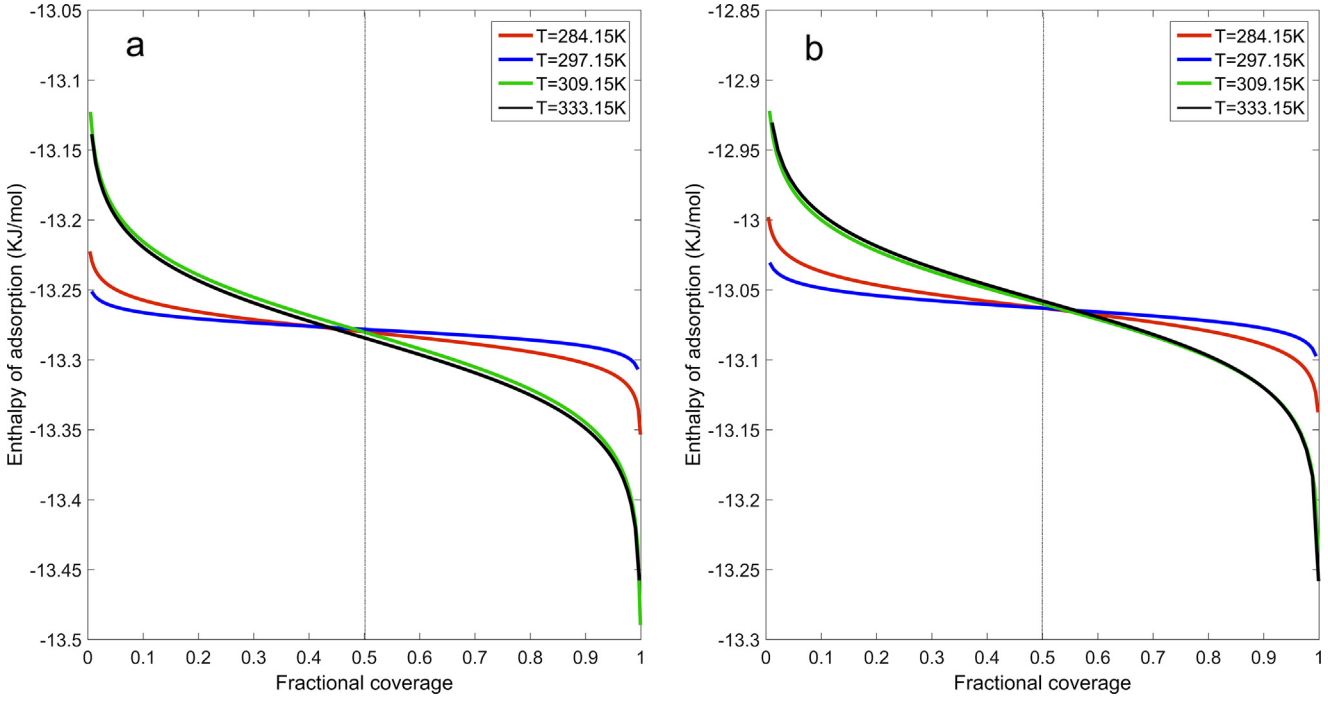

Fig. 5. Estimated values for isosteric enthalpy of ethyl acetate adsorption (based on Sips model) versus fractional coverage; (a) adsorption on Sepabeads SP20SS (b) Adsorption on Amberlite XAD16N.

predicting the adsorption behavior for high hydrophobic components with higher accuracy, however for prediction of isosteric enthalpy, this model is only applicable in intermediate range of concentrations, as discussed in Section 3.2.2.2, and at low concentration range, and loading close to zero, it cannot predict the isosteric enthalpy with high accuracy, therefore this model is only used for prediction of the isosteric enthalpy for ethyl acetate which is less hydrophobic and calculated values based on Sips prediction are compared with Langmuir model only for this ester component, and for the other three esters which are highly hydrophobic with equilibrium concentrations close to zero, Langmuir approach is used to predict the thermodynamic parameters. For the obtained isotherms at different four temperatures for ethyl acetate, as illustrated in Fig. 1, the values of maximum capacity q_{max}, k_0, n_0, α, and Q, are regressed based on the equations presented in Section 3.2.2.2 from the temperature dependent affinity and n parameters. The estimated values are assembled in Table 3. The standard error for each estimated parameter is obtained from correlation matrix R, corresponding to covariance matrix C and values of standard deviation sigma are obtained for each regressed parameter, for both adsorption on Sepabeads SP20SS and Amberlite XAD16N.

Based on the estimated values, reported in Table 3, fractional coverage (θ) is plotted versus enthalpy of adsorption as explained in Eq. (11), for four tested temperatures and for the two tested resins, shown in Fig. 5. As can be observed from enthalpy curves at different temperatures, the value of enthalpy is higher at lower temperatures, where the maximum achieved adsorption capacity is higher, due to higher energy barrier that adsorbed molecules need to overcome, and the value of enthalpy decreases with increase in temperature.

At fractional coverage equal to 0.5, the value of isosteric enthalpy of adsorption will be equal for the four tested temperatures and this value is reported as the heat of adsorption, highlighted in Table 3. For adsorption on Sepabeads SP20SS, the value of isosteric enthalpy is obtained as −13.3 kJ/mol, while it has a lower value -13.1 kJ/mol on

Table 4
Calculated values for heat, entropy and Gibbs energy of adsorption.

	Adsorption on Sepabeads SP20SS						Adsorption on Amberlite XAD16N					
	ΔH (kJ mol^{-1})	ΔS (kJ (mol K)$^{-1}$)	ΔG (kJ mol^{-1})			R^2	ΔH (kJ mol^{-1})	ΔS (kJ. (mol K)$^{-1}$)	ΔG (kJ mol^{-1})			R^2
			284.15 K	297.15 K	309.15 K	333.15 K			284.15 K	297.15 K	309.15 K	333.15 K	
Ethyl acetate	−13.6	−0.011	−10.5	−10.3	−10.2	−9.9	0.999	−12.6	−0.009	−10.1	−9.9	−9.9	−9.7	0.993
Isopentyl acetate	−25.0	−0.015	−21.2	−21.0	−20.8	−20.4	0.986	−20.3	−0.005	−18.8	−18.7	−18.7	−18.5	0.997
Ethyl 4-methylpentanoate	−28.1	−0.008	−25.9	−25.8	−24.7	−25.5	0.987	−21.1	−0.175	−22.4	−20.1	−18.0	−13.8	0.914
Ethyl hexanoate	−30.7	−0.023	−22.5	−22.1	−21.7	−21.1	0.997	−31.1	−0.028	−23.1	−22.7	−22.4	−21.7	0.989

Amberlite XAD16N. The isosteric enthalpy predicted based on Langmuir model is −13.6 kJ/mol which considering the range of standard error, falls in the same range as is predicted by Sips model, and the value predicted based on Langmuir model for adsorption on XAD16N, is −12.6 kJ/mol which is less than the value predicted by the Sips model.

The difference in prediction is caused by the more accurate estimation of the maximum capacity, applying the Sips model, as is also illustrated in Fig. 1. Although this model gives a more accurate prediction of maximum capacity at higher concentrations, it has application only in low concentration range, as explained in previous sections, therefore Langmuir model is used for calculation of thermodynamic parameters, Gibbs energy and entropy of adsorption.

4.1.3. Calculated Gibbs energy (ΔG^0) and entropy (ΔS^0) of adsorption

The maximum capacity is dependent on temperature, as can be observed from the obtained isotherms shown in Fig. 1. If the q_{max} decreases with temperature, the isosteric enthalpy increases with the loading, and it will reach a finite value when $\theta \rightarrow 1$ The Langmuir expression explained in Section 3.2.1.1 and the estimated heats of adsorption are used to predict the values of Gibbs energy and entropy of adsorption, based on Eqs. (13) and (14). The estimated values are reported in Table 4 for adsorption on Sepabeads SP20SS and Amberlite XAD16N, respectively.

The values for heat of adsorption, increase with the hydrophobicity of the ester component, and greater value for higher hydrophobic components such as ethyl hexanoate in comparison to ethyl acetate, implies that this compound interacts more with the resin material and higher energy is required that this component leaves the adsorbed phase after adsorption. Higher negative value for entropy of adsorption for this compound indicates that after adsorption this component is more stabilized on the adsorbent surface and it is more difficult to elute this component from the resin due to stronger binding in comparison to ethyl acetate, and the other less hydrophobic tested esters and molecules are more ordered on the adsorbent surface after adsorption. Comparing the values for Gibbs energy of adsorption, a decrease is observed in the estimated values with increase in temperature. The Gibbs energy of adsorption, as explained in Section 3.2.3 shows the degree of spontaneity of the adsorption and if the adsorption is favorable. The higher negative value indicates a more favorable adsorption and as it can be observed from the estimated values, the value of Gibbs energy of adsorption decreases with increase in temperature, which indicates that a temperature increase is not favorable for adsorption due to the exothermic nature of the adsorption phenomena. For physical adsorption to occur, the Gibbs energy of adsorption is between (−20 to 0 kJ/mol) [48], while it lies between (−80 to −400 kJ/mol) [48] if chemisorption is dominant. The estimated value of $\Delta G^0$for ethyl acetate is approximately −10.5 kJ/mol, whereas it is above −20 kJ/mol for the other three hydrophobic compounds adsorbed on Sepabeads SP20SS. The presented values demonstrate that for ethyl acetate physisorption is dominant and molecules bind to the surface of the adsorbent, and for the other three esters which has higher hydrophobicity and affinity towards the resin surface, molecules bind stronger to the adsorbent and Gibbs energy of adsorption equal or higher than −20 kJ/mol is obtained for most of the tested temperatures for high hydrophobic components, i.e. ethyl 4-methylpentanoate and ethyl hexanoate. Comparing the calculated values of ΔH^0 and ΔG^0 for adsorption on Sepabeads SP20SS, with the results obtained on XAD16N, it can be observed that a lower value is calculated for adsorption on XAD16N, mainly for ethyl acetate, isopentyl acetate, and ethyl 4-methylpentanoate, and it is due to the higher affinity of the Sepabeads SP20SS resin towards the tested esters and more spontaneous reaction on the surface of this resin in comparison.

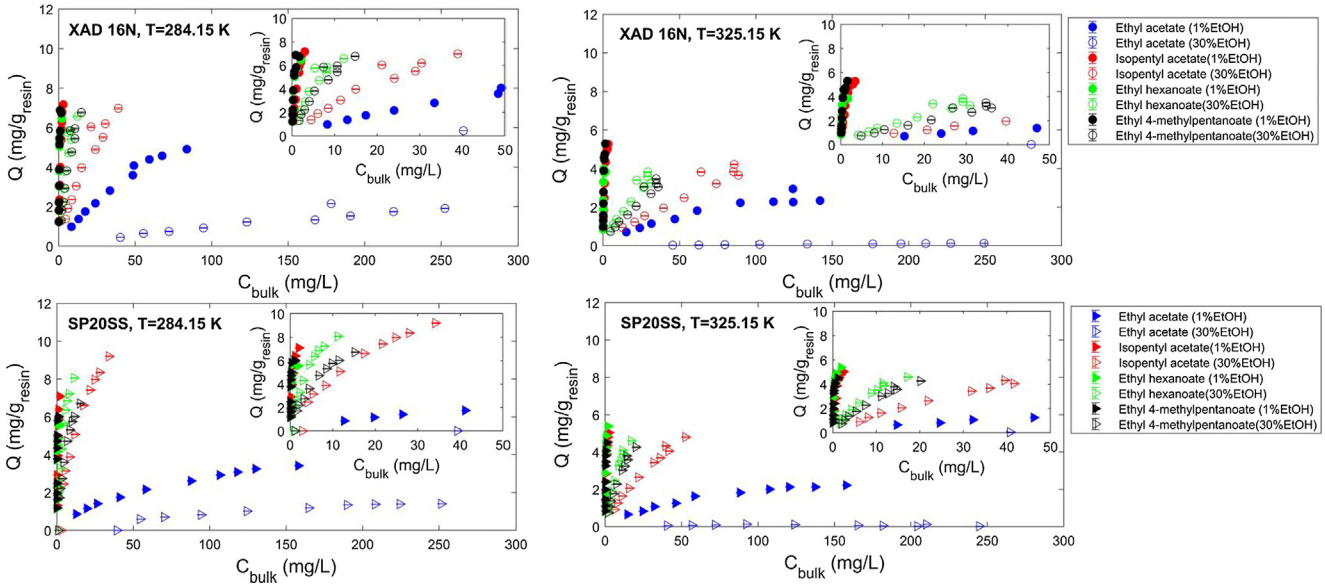

Fig. 6. Multicomponent adsorption isotherms; adsorption on XAD16N and on Sepabeads SP20SS (T = 284.15 and 325.15 K).

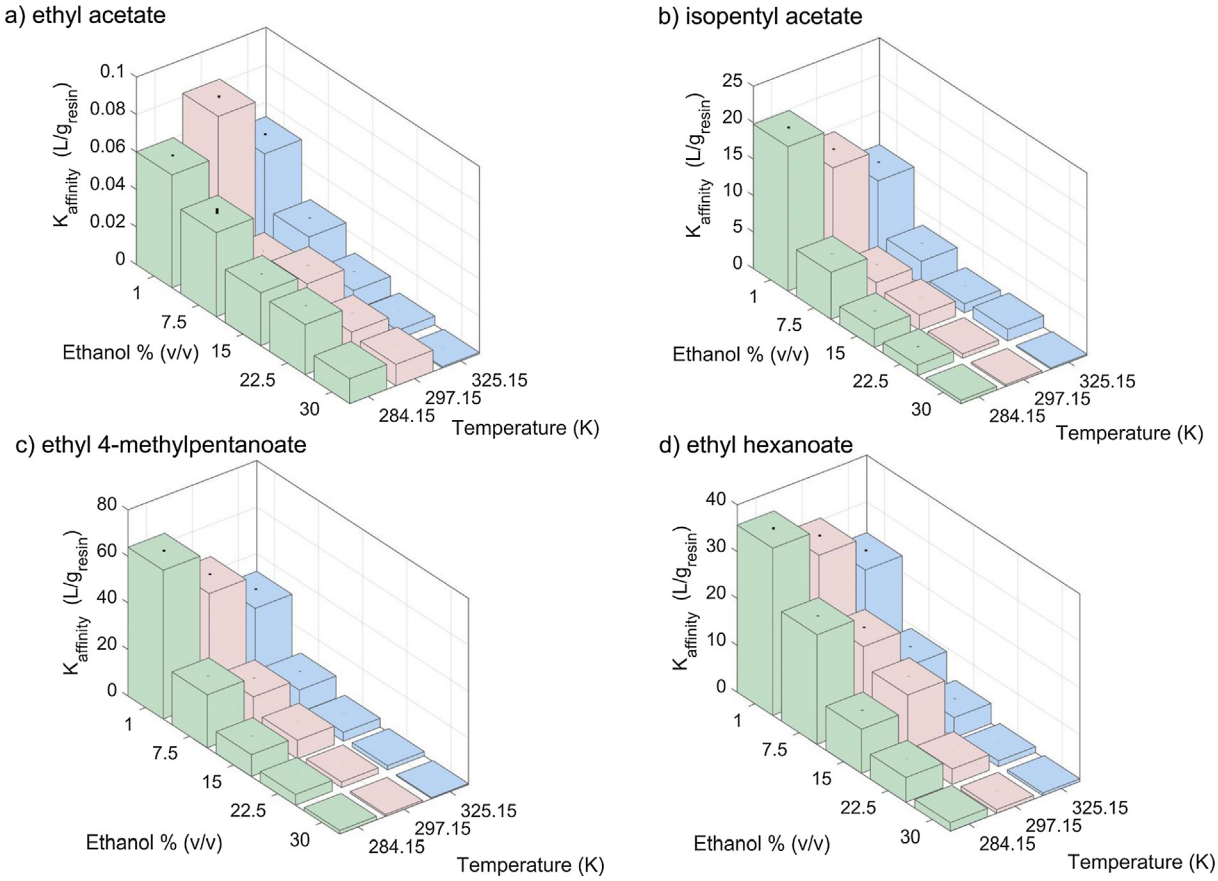

Fig. 7. $K_{affinity}$ as function of temperature and ethanol concentration, adsorption on Sepabeads SP20SS; (a) ethyl acetate, (b) isopentyl acetate, (c) ethyl 4-methylpentanoate, (d) ethyl hexanoate.

4.2. Influence of temperature and ethanol concentration on multicomponent adsorption

4.2.1. Effect of ethanol and temperature on $K_{affinity}$

The influence of temperature and ethanol concentration is investigated on multicomponent adsorption of the four aforementioned flavor-active esters as explained in Section 3.4.2. Multicomponent isotherms are obtained at the tested conditions for each flavor-active ester in the mixture, and for adsorption on the two tested resins. In order to compare the influence of tested conditions on equilibrium concentrations, and shape of the isotherms, the obtained isotherms for the tested conditions (temperatures 284.15, and 325.15 K), and ethanol concentrations (1 and 30% ethanol) are compared for each ester in the mixture and for each tested resin, depicted in Fig. 6.

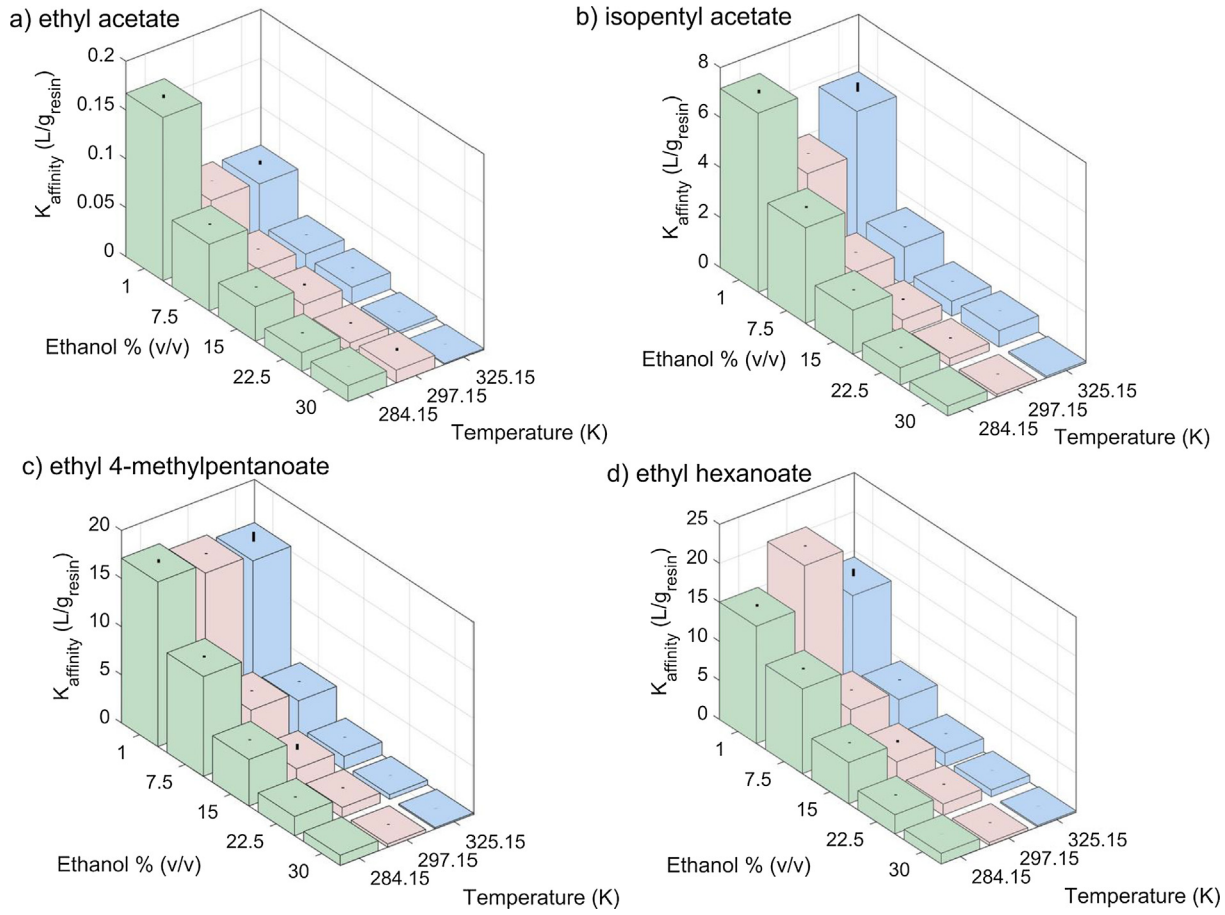

Fig. 8. $K_{affinity}$ as function of temperature and ethanol concentration, adsorption on Amberlite XAD16N; (a) ethyl acetate, (b) isopentyl acetate, (c) ethyl 4-methylpentanoate, (d) ethyl hexanoate.

Comparing the two figures at the top, it can be concluded that increase in temperature from 284.15 to 325.15 K, has higher influence on decrease of equilibrium binding capacity, at higher tested ethanol concentration, i.e. 30% ethanol. This influence is more significant for the decrease of equilibrium binding capacity for ethyl acetate, the more polar component in the mixture. Increase of both temperature and concentration of ethanol reveal a significant decrease in equilibrium binding capacity (approximately 93%), compared to 40% reduction at lower temperature (i.e. 284.15 K), and lower ethanol concentration (i.e. 1% v/v ethanol) for this ester. Similar behavior is observed for adsorption on Sepabeads SP20SS, according to the results presented in figures at the bottom. Higher reduction in equilibrium binding capacity (approximately 92%) was observed for ethyl acetate at higher tested temperature compared to 30% reduction at lower temperature. The comparison of results obtained for adsorption in the same tested conditions for the two tested resins, reveal a higher affinity towards more hydrophobic components ethyl hexanoate, ethyl 4-methylpentanoate, and isopentyl acetate in comparison to ethyl acetate, for the tested resin Sepabeads SP20SS. This resin has smaller particle size (between 50 and 100 μm) [43] compared to XAD16N with particle size (between 560 and 710 μm) [44], and has high surface area per volume. Moreover, larger pore volume for this resin as mentioned earlier, aids the diffusion of highly hydrophobic esters. Subsequently lower adsorption of ethyl acetate was observed for adsorption on this resin and for all the tested conditions. Due to lower hydrophobic nature and more polarity, separation of this component will be easier from the mixture in comparison to other tested components with higher hydrophobicity. The two components ethyl hexanoate and ethyl 4-methylpentanoate, with similar molecular structure and hydrophobicity, show similar adsorption behavior and strong binding and separation of these two components from each other can be challenging.

The experimental isotherms, obtained at all the tested conditions, presented in Section 3.4.2, are expressed with multicomponent Langmuir model and the thermodynamic parameters q_{max} and $k_{ads,i}$, explained in Section 3.2.4.1, are regressed, as explained in Eq. (15). The value of affinity parameter $K_{affinity}$ (L/g_{resin}) is calculated for all the tested conditions, i.e. tested temperatures and ethanol concentrations. The calculated values for $K_{affinity}$ are shown in Figs. 7 and 8 for adsorption on Sepabeads SP20SS and Amberlite XAD16N respectively. The error bars shown in the figures, are the standard errors calculated based on the diagonal of the covariance matrix estimated from the Jacobian given by the fitting function [14].

The values of $K_{affinity}$ presented in Figs. 7 and 8 confirm the strong binding of tested esters to the resin Sepabeads SP20SS in comparison to Amberlite XAD16N, which can be explained by the physical nature of the adsorbents, as discussed earlier.

As it can be detected from Figs. 7 and 8, increase in concentration of ethanol from 1 to 30% (v/v) has influence on the affinity parameter, as a considerable decrease in the value of $K_{affinity}$ was observed for all of the tested esters present in the mixture. With the increase of the ethanol concentration, the activity coefficient of esters in the mixture will decrease, and esters will have less tendency to leave the aqueous solution, therefore according to equality of chemical potential for component i in adsorbed and liquid phase, the affinity parameter can be described as a function of activity coefficient in the liquid phase. As the activity coefficient for esters decreases with increase in ethanol concentration, lower value for affinity parameter and subsequently lower binding capacity is expected to be obtained. Increase of temperature from

284.15 K to 325.15 K, showed a slight decrease in maximum capacities, due to exothermic nature of the adsorption, and as a result, lower value of $K_{affinity}$ is obtained at higher temperatures.

5. Conclusions

The result of this study performed for both single and multi-component adsorption of flavor-active esters on the two tested resins, show that equilibrium binding capacity is influenced to a great extent by increase in temperature and ethanol concentration. The estimated thermodynamic properties, give a better understanding of the adsorption behavior of each flavor-active ester present in the mixture (if the adsorption is dominated by physical or chemical adsorption) and for adsorption on the two tested resins. As these properties were not previously calculated for the adsorption of studied esters on these resins and studies in this regard, which are reported in the literature, are scarce, the estimated values for heat of adsorption contribute to our understanding of the adsorption phenomena for these components. The obtained Langmuir affinity parameters at various tested temperatures and ethanol concentrations for a multicomponent mixture, together with the estimated values for heat of adsorption, can be used as required parameters and can have further application in designing an adsorption column for separation of flavor-active esters in order to consider the non-isothermal condition for their separation.

Acknowledgements

This research work took place in the framework of ISPT (Institute of Sustainable Process Technology), under the grant number FO-10-05. We would like to acknowledge ISPT for its support and also thank Heineken Supply Chain for valuable comments.

Appendix A. Supplementary material

Supplementary data associated with this article can be found, in the online version, at https://doi.org/10.1016/j.seppur.2018.05.026.

References

[1] K.J. Verstrepen, G. Derdelinckx, J.-P. Dufor, J. Winderickx, J.M. Thevelein, I.S. Pretorius, F.R. Delvaux, Flavor-active esters: adding fruitiness to beer, J. Biosci. Bioeng. 96 (2003) 110–118.
[2] M.C. Meilgaard, The flavor of beer, MBAA Tech. Quart. 28 (1991) 132–141.
[3] M.C. Meilgaard, Flavor chemistry of beer. Flavor interaction between principal volatiles, MBAA Tech. Quart. 12 (1975) 107–117.
[4] T. Horak, J. Culik, V. Kellner, M. Jurkova, P. Cejka, D. Haskova, J. Dvorak, Analysis of selected esters in beer comparison of solid-phase microextraction and stir bar sorptive extraction, J. Inst. Brewing 116 (2010) 81–85.
[5] E.J. Pires, J.A. Teixeira, T. Branyik, A.A. Vicente, Yeast: the soul of beer's aroma-a review of flavour-active esters and higher alcohols produced by the brewing yeast, Appl. Microbiol. Biotechnol. 98 (2014) 1937–1949.
[6] D. Saison, D.P. De Schutter, B. Uyttenhove, F. Delvaux, F.R. Delvaux, Contribution of staling compounds to the aged flavour of lager beer by studying their flavour thresholds, Food Chem. 114 (2009) 1206–1215.
[7] L. Hiralal, A.O. Olaniran, B. Pillay, Aroma-active ester profile of ale beer produced under different fermentation and nutritional conditions, J. Biosci. Bioeng. 117 (2014) 57–64.
[8] C. Andrés-Iglesias, J. García-Serna, O. Montero, C.A. Blanco, Simulation and flavor compound analysis of dealcoholized beer via one-step vacuum distillation, Food Res. Int. 76 (2015) 751–760.
[9] T. Branyik, A.A. Vicente, P. Dostalek, J.A. Teixeira, A review of flavour formation in continuous beer fermentations, J. Inst. Brewing 114 (2008) 3–13.
[10] A.O. Olaniran, L. Hiralal, M.P. Mokoena, B. Pillay, Flavour-active volatile compounds in beer: production, regulation and control, J. Inst. Brewing 123 (2017) 13–23.
[11] A.G.H. Lea, J.R. Piggott, Fermented Beverage Production, Kluwer academic/Plenum Publishers, USA, 2003.
[12] S. Torres, M.D. Baigori, S.L. Swathy, A. Pandey, G.R. Castro, Enzymatic synthesis of banana flavour (isoamyl acetate) by bacillus licheniformis S-86 esterase, Food Res. Int. 42 (2009) 454–460.
[13] G.A.F. Harrison, The flavour of beer – a review, J. Inst. Brewing 76 (1970) 486–495.
[14] S. Saffarionpour, D.M. Mendez Sevillano, L.A.M. Van der Wielen, T.R. Noordman, M. Ottens, Selective adsorption pf flavor-active components on hydrophobic resins, J. Chromatogr. A 1476 (2016) 25–34.
[15] D.D. Duong, Adsorption Analysis: Equilibria and Kinetics, Imperial College Press, London, 1998.
[16] D.M. Ruthven, Principles of Adsorption and Adsorption Processes, John Wiley & Sons Inc., USA, 1984.
[17] R. Sips, On the structure of a catalyst surface, J. Phys. Chem. 16 (1948) 490–495.
[18] K.S.W. Sing, F. Rouquerol, J. Rouquerol, Classical interpretation of physisorption isotherms at the gas-solid interface, in: J. Rouquerol, F. Rouquerol, P. Liewellyn, G. Maurine, G.M.K. Sing (Eds.) Adsorption by Powders and Porous Solids, Principles, Methodology, and Applications, Elsevier Ltd., 2014.
[19] D.D. Do, D. Nicholson, H.D. Do, On the Henry constant and isosteric heat at zero loading in gas phase adsorption, J. Colloid Interface Sci. 324 (2008) 15–24.
[20] F.N. Ridha, P.A. Webley, Entropic effects and isosteric heats of nitrogen and carbon dioxide adsorption on chabazite zeolites, Microporous Mesoporous Mater. 132 (2010) 22–30.
[21] F. Gritti, G. Guiochon, Isosteric heat of adsorption in liquid–solid equilibria: theoretical determination and measurement by liquid chromatography/mass spectrometry, J. Chromatogr. A 1216 (2009) 4645–4751.
[22] J.M. Prausnitz, Molecular thermodynamics: opportunities and responsibilities, Fluid Phase Equilib. 116 (1996) 12–26.
[23] A. Seidel-Morgenstern, G. Guiochon, Thermodynamics of the adsorption of Troger's base enantiomers from ethanol on cellulose triacetate, J. Chromatogr. A 631 (1993) 37–47.
[24] S. Builes, S.I. Sandler, R. Xiong, Isosteric heats of gas and liquid adsorption, Langmuir 29 (2013) 10416–10422.
[25] R.K. Tadapaneni, R. Yang, B.T. Carter, J. Tang, A new method to determine the water activity and the net isosteric heats of adsorption for low moisture foods at elevated temperatures, Food Res. Int. 102 (2017) 203–212.
[26] H. Kim, G. Guiochon, Thermodynamic functions and intraparticle mass transfer kinetics of structural analogues of a template on molecularly imprinted polymers in liquid chromatography, J. Chromatogr. A 1097 (2005) 84–97.
[27] R. Überbacher, A. Rodler, R. Hahn, A. Jungbauer, Hydrophobic interaction chromatography of proteins: thermodynamic analysis of conformational changes, J. Chromatogr. A 1217 (2010) 184–190.
[28] M. Barkat, D. Nibou, S. Chegrouche, A. Mellah, Kinetics and thermodynamics studies of chromium(VI) ions adsorption onto activated carbon from aqueous solutions, Chem. Eng. Process. Process Intensif. 48 (2009) 38–47.
[29] B.H. Hameed, A.A. Ahmad, N. Aziz, Isotherms, kinetics and thermodynamics of acid dye adsorption on activated palm ash, Chem. Eng. J. 133 (2007) 195–203.
[30] H. Nollet, M. Roels, P. Lutgen, P. Van der Meeren, W. Verstraete, Removal of PCBs from wastewater using fly ash, Chemosphere 53 (2003) 655–665.
[31] D.A. Kulik, Standard molar Gibbs energies and activity coefficients of surface complexes on mineral water interfaces (Thermodynamic insights), in: J. Lützenkirchen (Ed.), Interface Science and technology, Elsevier Ltd., 2006.
[32] I.A.W. Tan, B.H. Hameed, A.L. Ahmad, Equilibrium and kinetic studies on basic dye adsorption by oil palm fibre activated carbon, Chem. Eng. J. 127 (2007) 111–119.
[33] V. Gokmen, A. Serpen, Equilibrium and kinetic studies on the adsorption of dark colored compounds from apple juice using adsorbent resin, J. Food Eng. 53 (2002) 221–227.
[34] T. Sarvinder Singh, K.K. Pant, Equilibrium, kinetics and thermodynamic studies for adsorption of As (III) on activated alumina, Sep. Purif. Technol. 36 (2004) 139–147.
[35] I.A. Tan, A.L. Ahmad, B.H. Hameed, Adsorption isotherms, kinetics, thermodynamics and desorption studies of 2,4,6-trichlorophenol on oil palm empty fruit bunch-based activated carbon, J. Hazard. Mater. 164 (2009) 473–482.
[36] L. Yanxu, C. Jiangyo, S. Yinghuang, Adsorption of multicomponent volatile organic compounds on semi-coke, Carbon 46 (2008) 858–863.
[37] G. Storti, M. Masi, S. Carra, M. Morbidelli, Optimal design of multicomponent countercurrent adsorption separation processes involving nonlinear equilibria, Chem. Eng. Sci. 44 (1989) 1329–1345.
[38] M. Mazzotti, G. Storti, M. Morbidelli, Shock layer analysis in multicomponent chromatography and countercurrent adsorption, Chem. Eng. Sci. 49 (1994) 1337–1355.
[39] M. Kaspereit, A. Seidel-Morgenstern, Process concepts in preparative chromatography, in: S. Fanali, P.R. Haddad, C. Poole, P. Schoenmakers, D.K. Lioyd (Eds.), Liquid Chromatography, Fundamentals and Instrumentation, Elsevier Inc., USA, 2013.
[40] K. Abburi, Adsorption of phenol and p-chlorophenol from their single and bisolute aqueous solutions an Amberlite XAD-16 resin, J. Hazard. Mater. 105 (2003) 143–156.
[41] https://www.chemaxon.com/ (accessed 28 June, 2017).
[42] K.Y. Foo, B.H. Hameed, Insights into modeling of adsorption isotherm systems, Chem. Eng. J. 156 (2010) 2–10.
[43] SP20SS, in, Sigma Aldrich. https://www.sigmaaldrich.com/catalog/product/supelco/13617u?lang=en&region=NL (accessed 5 April, 2018).
[44] XAD16N, Sigma Aldrich, https://www.sigmaaldrich.com/catalog/product/sigma/xad16?lang=en&region=NL, (accessed 5 April, 2018).
[45] D. Xue, Y. Chen, Solving Applied Mathematical Problems with MATLAB, CRC Press, Taylor & Francic Group I.I.C., 2008.
[46] E. Zondervan, A Numerical Primer for the Chemical Engineer, in, CRC Press, Taylor & Francic Group, 2015.
[47] Y. Liu, Y.-J. Liu, Biosorption isotherms, kinetics and thermodynamics, Sep. Purif. Technol. 61 (2008) 229–242.
[48] S.E. Agarry, O.O. Oguneleye, O.A. Ajani, Biosorptive removal of Cadmium (II) ions from aqeous solution by chemically modified onion skin: batch equilibrium, kinetic and thermodynamic studies, Chem. Eng. Commun. 202 (2015) 655–673.